Persistent spin squeezing of a dissipative one-axis twisting model embedded in a general thermal environment

Yong-Hong Ma,[1,2,*] Quan-Zhen Ding,[2] and Ting Yu[2,†]

[1]*School of Science, Inner Mongolia University of Science and Technology, Baotou 014010, People's Republic of China*

[2]*Department of Physics and Center for Quantum Science and Engineering, Stevens Institute of Technology, Hoboken, New Jersey 07030, USA*

(Received 23 July 2019; accepted 27 January 2020; published 21 February 2020)

We investigate spin squeezing for a one-axis twisting (OAT) model coupled to a general non-Markovian environment in a finite-temperature regime. Using the non-Markovian quantum state diffusion and master equation approach, we numerically study non-Markovian spin-squeezing generation in the OAT model. Our results show that the total spin number N, energy k_BT, and certain coefficients in the OAT model can play a crucial role in generating spin squeezing. In particular, it shows that the maximum spin squeezing can be significantly enhanced when the participating environment has a relatively long memory time.

DOI: 10.1103/PhysRevA.101.022327

I. INTRODUCTION

Spin squeezing, as an important quantum resource, has many potential applications in quantum science and technology such as quantum metrology, atom interferometers [1–5], and quantum information processing due to its close relation with quantum entanglement [6–11]. A spin-squeezing state is defined for an ensemble of spins whose fluctuation in one collective spin direction to the mean spin direction is smaller than the classical limit [2]. The growing interest in studying spin squeezing [2] has arisen mainly from exploring the correlation and many-body entanglement [12–14] of particles, especially for the purpose of improving measurement precision [1,15–19].

As pointed out by Kitagawa and Ueda [2], the spin-squeezing states can be generated via two main methods: the OAT model and two-axis countertwisting (TACT) model. At present, a number of methods to generate spin squeezing in atomic systems have been proposed and successfully realized, including the transfer of squeezing property from light to matter and quantum nondemolition measurement of atomic states [4,5,20–27]. In the past decade, different techniques of preparing high-quality spin-squeezed states have been widely studied in many interesting physical systems, including nuclear spins [28,29], nitrogen-vacancy (NV) centers [30–32], and electron spins [33], to name a few.

A realistic analysis of spin squeezing must take into account decoherence and dissipation phenomena. The theoretical descriptions of spin squeezing in the open-system context are mostly considered under Born-Markov approximations due to their simplicity in deriving Markov dynamical equations and the interest in the long-time limit. Generally, Markov Langevin equations or the corresponding master equations can be used to characterize the spin squeezing while the environment noises are taken as a weak perturbation and the memory effects are completely ignored [24,30,34–39]. Spin squeezing for N independent spin-$1/2$ particles under non-Markovian channels has been studied [40]. The information about squeezing processes in a wide range of time scales including short-time, mid-time, and long-time limits are needed in applications where the system of interest is embedded in an environment that exhibits a finite-time correlation. Non-Markovian features are crucial for many important physical processes involving strong system-environment interactions or long-range temporal correlations [41–43]. Moreover, when the open system is coupled to a structured reservoir, e.g., for quantum channels that are embedded in physical media such as band-gap crystals [44–46], the environmental memory effects cannot be ignored. In all these cases, the system dynamics can be substantially different from the Markov ones [47]. One of our motivations in this paper is to investigate how spin squeezing survives in the presence of non-Markovian relaxation on every site based on the OAT model. Our investigations involve the spin-squeezing generation in wide temporal domains and OAT model parameter ranges.

In this paper, we study the dynamics of spin squeezing of an OAT model constituted of N independent spin-$1/2$ particles coupled to a non-Markovian environment in a finite-temperature regime. We derive a non-Markovian master equation by using the quantum-state diffusion (QSD) approach [48–50]. Solving the time evolutions of several operator expectations, we find that open systems exhibiting strong non-Markovian features can substantially modify the dynamics of spin squeezing. More specifically, it shows that the environment memory time can significantly alter the speed of spin-squeezing generation. In addition, we show how to choose effective parameters to achieve the maximum squeezing.

The organization of material is as follows. In Sec. II we present the OAT model and give an effective model Hamiltonian. In Sec. III, we derive the master equation based on the non-Markovian quantum-state diffusion (NMQSD) equation. In Sec. IV the environmental memory effects on

*myh_dlut@126.com

†ting.yu@stevens.edu

spin squeezing are systematically investigated. We also give a careful description of how to achieve the maximum spin squeezing by tuning the key parameters of the OAT model. Finally, the conclusion is given in Sec. V. Some details about the equations of motions for the expectations are left to Appendix A.

II. HAMILTONIAN OF THE SYSTEM

An OAT model can be considered a specific case of Lipkin-Meshkov-Glick (LMG) model, which was initially introduced in nuclear physics [51] and has been widely used in many other fields in recent years, such as statistical mechanics of quantum spin systems [52], Bose-Einstein condensation [53], and superconducting circuits [54]. The Hamiltonian of a LMG model can be described as (setting $\hbar = 1$)

$$\begin{aligned}\hat{H}_{\mathrm{LMG}} &= -\frac{\lambda}{N}\sum_{i<j}\left(\sigma_x^i\sigma_x^j + \alpha\sigma_y^i\sigma_y^j\right) - h\sum_i \sigma_z^j \\ &= -\frac{2\lambda}{N}\left(J_x^2 + \alpha J_y^2\right) - 2hJ_z + \frac{\lambda}{2}(1+\alpha), \end{aligned} \tag{1}$$

where σ_β represents a Pauli matrix, $J_\beta = \sum_i \sigma_\beta^i/2$ is the collective spin operator (denoted as $J_z = \frac{1}{2}\sum_n(|1\rangle_n\langle 1| - |0\rangle_n\langle 0|)$, $J_x = \frac{1}{2}\sum_n(|1\rangle_n\langle 0| + |0\rangle_n\langle 1|)$, $J_+ = \sum_n |1\rangle_n\langle 0|$, $J_- = \sum_n |0\rangle_n\langle 1|$), and N is the total spin number. We can obtain several different forms of the LMG Hamiltonian by choosing suitable parameters. Generally, the anisotropic parameter α satisfies $0 \leqslant \alpha \leqslant 1$. Ma and Wang calculated the spin squeezing in the isotropic case ($\alpha = 1$) [55] in a Markov limit. In this paper, we consider the ferromagnetic case ($\lambda > 0$) and the isotropic case simultaneously. Thus, the effective Hamiltonian can be written as

$$\begin{aligned}\hat{H} &= -\frac{2\lambda}{N}\left(J_x^2 + J_y^2\right) - 2hJ_z + \lambda \\ &= -\frac{2\lambda}{N}\left(\mathbf{J}^2 - J_z^2\right) - 2hJ_z + \lambda,\end{aligned} \tag{2}$$

where $\mathbf{J}$ is the conserved quantity. The effective Hamiltonian can be simplified to an OAT Hamiltonian,

$$\hat{H}_{\mathrm{sys}} = aJ_z + bJ_z^2, \tag{3}$$

where $a = -2h$ and $b = \frac{2\lambda}{N}$.

III. NON-MARKOVIAN MASTER EQUATION AT FINITE TEMPERATURE

We start with this OAT model which interacts with a bosonic oscillator environment for the total Hamiltonian

$$H_{\mathrm{tot1}} = aJ_z + bJ_z^2 + \sum_j \omega_j b_j^\dagger b_j + \sum_j (g_j^* L^\dagger b_j + g_j L b_j^\dagger), \tag{4}$$

where ω_j, $b_j^\dagger$, and b_j are frequencies, creation operators, and annihilation operators of the heat bath, respectively, g_j are the coupling constants between the system and the bath, and the Lindblad operator $L = J_-$ here indicates spin damping. For the Hamiltonian H_{tot1}, we assume that the heat bath is initially in a thermal equilibrium state. Here we need to introduce a fictitious heat bath which has no interaction with either the system or the bath coupled to the system. The time evolution of the system is unaffected by this fictitious bath. The total Hamiltonian including two independent heat baths can be written as [56]

$$\begin{aligned}H_{\mathrm{tot2}} = aJ_z + bJ_z^2 + \sum_j \omega_j b_j^\dagger b_j + \sum_j (g_j^* L^\dagger b_j + g_j L b_j^\dagger) \\ - \sum_j \omega_j c_j^\dagger c_j,\end{aligned} \tag{5}$$

where c_j ($c_j^\dagger$) is the bosonic annihilation (creation) operator of the fictitious heat bath. We can do a boson Bogoliubov transformation by using two bosonic operators d_j and e_j,

$$b_j(c_j) = \sqrt{\bar{n}_j + 1}\, d_j(e_j) + \sqrt{\bar{n}_j}\, e_j^\dagger(d_j^\dagger), \tag{6}$$

where $\bar{n}_j = \frac{1}{\exp(\hbar\omega_j/k_B T) - 1}$ denotes the mean thermal occupation number of mode ω_j. After transformation, the new Hamiltonian for operators d_j and e_j is then given by [56]

$$\begin{aligned}H_{\mathrm{tot3}} = aJ_z + bJ_z^2 + \sum_j \sqrt{\bar{n}_j + 1}\,(g_j^* L^\dagger d_j + g_j L d_j^\dagger) \\ + \sum_j \omega_j d_j^\dagger d_j + \sum_j \sqrt{\bar{n}_j}\,(g_j^* L^\dagger e_j + g_j L e_j^\dagger) \\ - \sum_j \omega_j e_j^\dagger e_j.\end{aligned} \tag{7}$$

Therefore, we map the finite-temperature bath into two zero-temperature baths. The initial vacuum state can be expressed as $|0\rangle = |0\rangle_d \bigotimes |0\rangle_e$, with $d_j|0\rangle = 0$ and $e_j|0\rangle = 0$. Thus, the trajectory $\psi_t = |\psi_t(z^*, w^*)\rangle$ satisfies the following NMQSD equation with two independent noises z_t^* and w_t^* [56]:

$$\begin{aligned}\partial_t \psi_t = -iH_{\mathrm{sys}}\psi_t + Lz_t^*\psi_t - L^\dagger \int_0^t ds\, \alpha_1(t,s)\frac{\delta\psi_t}{\delta z_s^*} \\ + L^\dagger w_t^* \psi_t - L\int_0^t ds\, \alpha_2(t,s)\frac{\delta\psi_t}{\delta w_s^*},\end{aligned} \tag{8}$$

where

$$\begin{aligned}\alpha_1(t,s) &= \sum_j (\bar{n}_j + 1)|g_j|^2 e^{-i\omega_j(t-s)}, \\ \alpha_2(t,s) &= \sum_j \bar{n}_j |g_j|^2 e^{i\omega_j(t-s)},\end{aligned} \tag{9}$$

are the bath correlation functions. Two independent and complex Gaussian noises $z_t^* = -i\sum_j \sqrt{\bar{n}_j + 1}\, g_j^* z_j^* e^{i\omega_j t}$ and $w_t^* = -i\sum_j \sqrt{\bar{n}_j}\, g_j^* w_j^* e^{-i\omega_j t}$ satisfy $\mathcal{M}[z_t] = \mathcal{M}[z_t z_s] = 0$, $\mathcal{M}[z_t^* z_s] = \alpha_1(t,s)$, $\mathcal{M}[w_t] = \mathcal{M}[w_t w_s] = 0$, and $\mathcal{M}[w_t^* w_s] = \alpha_2(t,s)$. The expression $\mathcal{M}[\cdot] = \int \frac{dz^2}{\pi} e^{-|z|^2} \int \frac{dw^2}{\pi} e^{-|w|^2}[\cdot]$ describes the statistical mean over the Gaussian processes z_t^* and w_t^*. The stochastic Schrödinger equation (8) can be greatly simplified by using two time-dependent operators O_1 and O_2, which satisfy $\frac{\delta\psi_t}{\delta z_s^*} = O_1(t,s,z^*,w^*)\psi_t$ and $\frac{\delta\psi_t}{\delta w_s^*} = O_2(t,s,z^*,w^*)\psi_t$ [56]. Thus, the NMQSD equation can be written as

$$\begin{aligned}\partial_t \psi_t = -iH_{\mathrm{sys}}\psi_t + Lz_t^*\psi_t - L^\dagger \bar{O}_1(t,z^*,w^*)\psi_t \\ + L^\dagger w_t^*\psi_t - L\bar{O}_2(t,z^*,w^*)\psi_t,\end{aligned} \tag{10}$$

where $\bar{O}_i$ $(i=1,2)$ is expressed as $\bar{O}_i(t,z^*,w^*)=\int_0^t \alpha_i(t,s)O_i(t,s,z^*,w^*)\,ds$ $(i=1,2)$. In an integral representation, the two correlation functions at finite temperature are

$$\alpha_1(t,s)=\int d\omega\left(\frac{1}{e^{\omega/k_BT}-1}+1\right)J(\omega)e^{-i\omega(t-s)},$$
$$\alpha_2(t,s)=\int d\omega\frac{1}{e^{\omega/k_BT}-1}J(\omega)e^{i\omega(t-s)}. \quad (11)$$

Their decay, as functions of the time delay $t-s$, defines the memory or correlation time of the environment. In the following content, we introduce a Lorentz-Drude spectral density: $J(\omega)=\frac{\Gamma}{\pi}\frac{\omega}{1+\omega^2/\gamma^2}$ with a decay rate Γ. The two correlation functions are linear at low frequencies, and decay as $1/\omega$ beyond the cutoff γ. In the high-temperature limit $k_BT\gg a(b)$, Eq. (11) reduces to

$$\alpha_1(t,s)=k_BT\Gamma\Lambda(t,s)+i\Gamma\frac{\partial\Lambda(t,s)}{\partial t},$$
$$\alpha_2(t,s)=k_BT\Gamma\Lambda(t,s), \quad (12)$$

where $\Gamma\Lambda(t,s)=\Gamma\frac{\gamma}{2}e^{-\gamma|t-s|}$ is an Ornstein-Uhlenbeck correlation function with the environmental memory time $1/\gamma$. For a large cutoff γ, the non-Markovian environment goes back to the Markov case. This is the well-known Caldeira-Leggett (CL) limit $k_BT\gg\gamma\gg a(b)$. Note that Eq. (12) is only valid in high-temperature cases for recovering the Markov case. We use Eq. (10) rather than Eq. (12) for our simulations in the following content. For the purpose of solving Eq. (10), we need to determine the operators O_1 and O_2. Generally, O operators can be obtained by invoking a perturbation technique [49,50]. By using the consistency conditions $\partial_t\frac{\delta\psi_t}{\delta z_s^*}=\frac{\delta}{\delta z_s^*}\partial_t\psi_t$ and $\partial_t\frac{\delta\psi_t}{\delta w_s^*}=\frac{\delta}{\delta w_s^*}\partial_t\psi_t$, in the regime $K_BT\Gamma\ll a(b)$, two operators O_1 and O_2 satisfy the following equations (as detailed in Appendix A):

$$\partial_tO_1(t,s)=[-iH_{\rm sys}-L^\dagger\bar{O}_1-L\bar{O}_2,O_1]\quad(L=J_-),$$
$$\partial_tO_2(t,s)=[-iH_{\rm sys}-L^\dagger\bar{O}_1-L\bar{O}_2,O_2], \quad (13)$$

with

$$O_1=f_{11}(t,s)J_-+f_{12}(t,s)J_zJ_-,$$
$$O_2=f_{21}(t,s)J_++f_{22}(t,s)J_+J_z, \quad (14)$$

where f_{ij} $(i,j=1,2)$ is a time-dependent coefficient. To get more information about these coefficients, we substitute Eq. (14) into Eq. (13), ignoring high-order terms $J_+^mJ_z^n$ $(m+n\geqslant3)$ or $J_z^nJ_-^m$ $(m+n\geqslant3)$; the differential equations of the coefficients in the O_1 and O_2 operators can be derived by

$$\partial_tf_{11}=f_{11}\left\{ia+ib+J\left(J-\frac{1}{2}\right)F_{12}-2F_{21}+\left(J\left(J-\frac{1}{2}\right)-2\right)F_{22}\right\}+f_{12}\left(ibJ-JF_{11}+\frac{J}{2}F_{12}-JF_{21}-\frac{5}{2}JF_{22}\right), \quad (15)$$

$$\partial_tf_{12}=f_{11}\{2ib-2F_{11}+F_{12}-2F_{21}-5F_{22}\}+f_{12}\left\{ia+ib+\left(J(J+1)-3\left(\frac{3}{2}J-\frac{1}{2}\right)\right)F_{12}-2F_{21}+\left(J(J+1)-2-3\left(\frac{3}{2}J-\frac{1}{2}\right)\right)F_{22}\right\}, \quad (16)$$

$$\partial_tf_{21}=-f_{21}\{ia+ib+J(J+1)F_{12}-2F_{21}+(J(J+1)-2)F_{22}\}, \quad (17)$$

$$\partial_tf_{22}=-f_{21}\{2ib-2F_{11}+F_{12}-2F_{21}-5F_{22}\}-f_{22}\{ia+ib+J(J+1)F_{12}-2F_{21}+(J(J+1)-2)F_{22}\}, \quad (18)$$

where the non-Markovian corrections F_{ij} can be expressed by $F_{ij}=\int_0^t ds\alpha_i(t,s)f_{ij}(t,s)$ $(i,j=1,2)$. The initial conditions for Eq. (15)–(18) are $f_{11}(t=s,s)=f_{21}(t=s,s)=1$ and $f_{12}(t=s,s)=f_{22}(t=s,s)=0$.

With the noise-free $\hat{O}_j$ operator in Eq. (10), by taking the statistical mean over noises, the master equation takes a very simple form [56]:

$$\partial_t\rho_t=-i[H_{\rm sys},\rho_t]+[L,\ \mathcal{M}\{P_t\bar{O}_1^\dagger(t,z^*,w^*)\}]-[L^\dagger,\ \mathcal{M}\{\bar{O}_1(t,z^*,w^*)P_t\}]+[L^\dagger,\ \mathcal{M}\{P_t\bar{O}_2^\dagger(t,z^*,w^*)\}]-[L,\ \mathcal{M}\{\bar{O}_2(t,z^*,w^*)P_t\}], \quad (19)$$

with the unnormalized projection operator $P_t=|\psi_t(z^*,w^*)\rangle\langle\psi_t(z^*,w^*)|$. The above equation is the general master equation at finite temperature. Note that this last result is still not a closed evolution equation for ρ_t. Following our previous result in Ref. [56], the closed master equation can be derived as

$$\partial_t\rho=-i[H_{\rm sys},\rho]+[L,\rho\bar{O}_1^\dagger(t)]+[\bar{O}_1(t)\rho,L^\dagger]+[L^\dagger,\rho\bar{O}_2^\dagger(t)]+[\bar{O}_2(t)\rho,L], \quad (20)$$

with

$$\bar{O}_1=F_{11}(t)J_-+F_{12}(t)J_zJ_-,$$
$$\bar{O}_2=F_{21}(t)J_++F_{22}(t)J_+J_z,$$
$$\bar{O}_1^\dagger=F_{11}^*(t)J_++F_{12}^*(t)J_+J_z,$$
$$\bar{O}_2^\dagger=F_{21}^*(t)J_-+F_{22}^*(t)J_zJ_-. \quad (21)$$

In Fig. 1 we show the time dependence of the coefficients F_{ij} $(i,j=1,2)$. For the correlation considered in this paper, it shows the transitions from the non-Markovian to the Markov case through the time evolution. We can clearly see that the non-Markovian environment changes the dynamical behavior in the early stage of the time evolution. However, in the Markov regime for the long-time evolution, the environment drives the system to the steady state. For a correlation function without steady states, the long-time non-Markovian behavior will be very different [57].

IV. SPIN SQUEEZING

In order to study spin squeezing of the present system in a non-Markovian environment, we employ the spin-squeezing

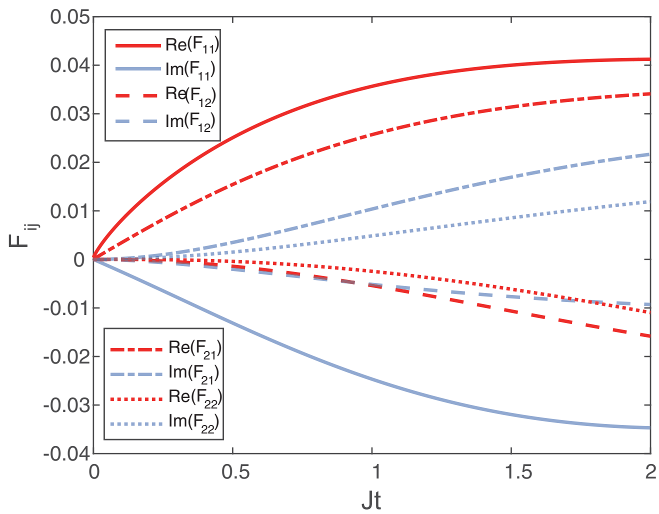

FIG. 1. Time evolution of the coefficients F_{ij} in the O operator. The parameters are $a = 1$, $b = -1$, $\Gamma = 0.01$, $\gamma = 5$, $kT = 10$, and $N = 10$.

parameter ξ^2 [15,58] to ascertain spin squeezing, which can be defined as

$$\xi^2 = \frac{N\langle \Delta J_{\min}^2 \rangle}{\langle J_x \rangle^2}, \tag{22}$$

where

$$\langle \Delta J_{\min}^2 \rangle = \frac{1}{2}\left(\langle J_y^2 + J_z^2 \rangle - \sqrt{\left(\langle J_y^2 - J_z^2 \rangle\right)^2 + 4\langle J_y J_z \rangle_{ss}^2}\right), \tag{23}$$

with $\langle J_y J_z \rangle_{ss} = \langle J_y J_z + J_z J_y \rangle/2$. There is spin squeezing when $\xi^2 < 1$. To create a spin-squeezed state, we initially prepare the ensemble in a coherent spin state along the x axis of the Block sphere. Thus the initial conditions are $\langle J_x \rangle = J$ (the conserved quantity $J = N/2$), $\langle J_y^2 \rangle = \langle J_z^2 \rangle = J$, and $\langle J_y \rangle = \langle J_z \rangle = 0$. By using the equations in Appendix B, we can numerically study non-Markovian spin-squeezing generation in this OAT model.

Figure 2(a) shows the evolution of the spin-squeezing parameter ξ^2 with different memory parameter γ. For $\gamma = 0.1$, corresponding to a relatively long memory time, the stronger spin squeezing with a long period can be generated, exemplifying strong non-Markovian effects. The degree of spin squeezing becomes weak with a short period as memory parameter γ is increased. Moreover, the part of the exponential decay for the non-Markovian process becomes a key element and the spin squeezing disappears finally, similar to the Markov decoherence case in the long-time limit. At $\gamma = 10$ where it nearly approaches the Markov regime, a relatively weak spin squeezing can be seen. In the Markov regime, a very weak spin squeezing can be seen that only lasts a short time period. The main reason is that the major decoherence agent is generally the amplitude damping; the environmental memory is the major determinant of slowing down the dissipative process due to the back-reaction or information backflow. Therefore, in order to get the strong and long-period spin squeezing, we hope that the dissipative dynamics can be temporally reversed and the lost energy or information can come back to the system due to the memory effect. However, for the Markov case, the environment causes the system to decay exponentially without the information backflow. Thus, a long memory time not only increases the degrees of the spin squeezing values but also helps to achieve the high spin-squeezing degrees in shorter time scales as well.

In Fig. 2(b), we plot the evolutions of spin-squeezing parameter ξ^2 with different spin numbers N for small $\gamma = 0.1$ corresponding to a long memory time at finite temperature. We see that the degree of spin squeezing grows with varying values of N, which agrees with the results in Ref. [30], where it is shown that the optimal squeezing degree is proportional to $\sqrt{N}$ (that is, $\xi^2 \simeq \frac{2}{\sqrt{J\eta}}$). Thus, relatively large spin numbers not only increase the maximum spin-squeezing

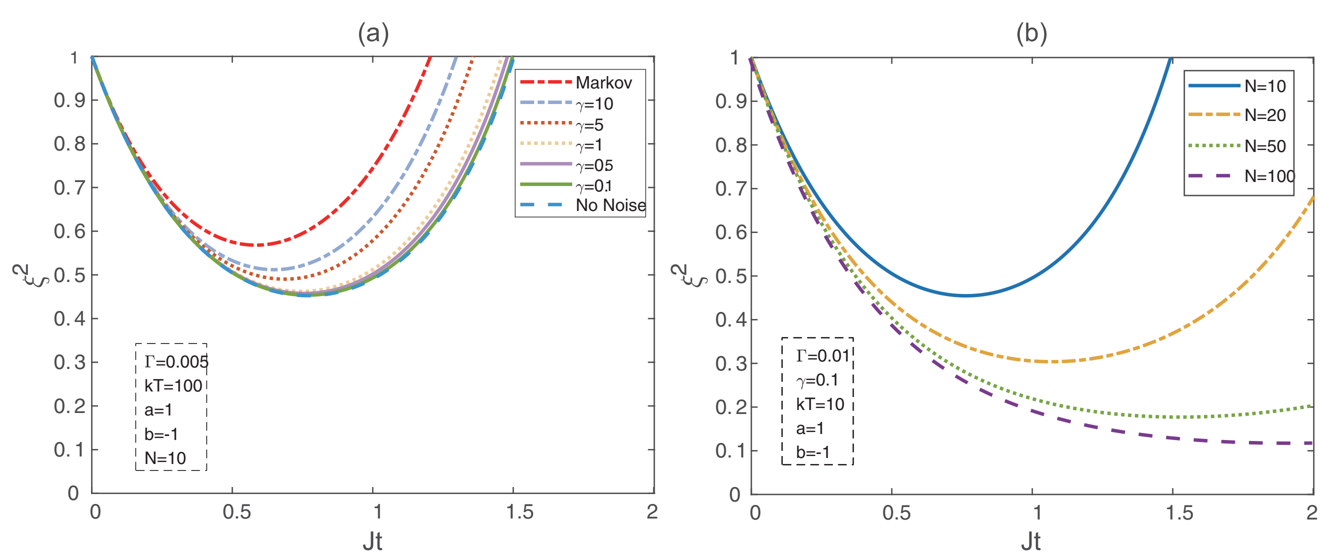

FIG. 2. The time evolution of the spin-squeezing parameter ξ^2 with (a) different memory parameter γ and (b) different spin number N. The parameters are (a) $\Gamma = 0.005$, $kT = 100$, $N = 10$, $a = 1$, and $b = -1$ with different memory parameter γ and (b) $\Gamma = 0.01$, $\gamma = 0.1$, $kT = 10$, $a = 1$, and $b = -1$ with different spin number N. Solid blue line, $N = 10$; dash-dotted orange line, $N = 20$; dotted green line, $N = 50$; and dashed purple line, $N = 100$.

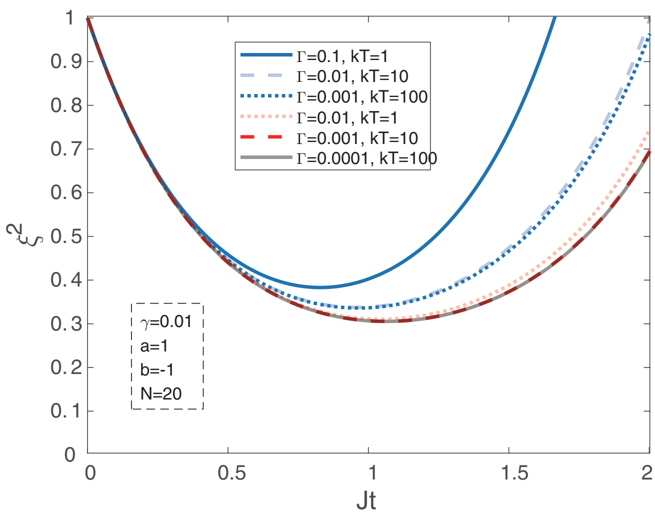

FIG. 3. The time evolution of spin-squeezing parameter ξ^2 with the different damping rate Γ and with the different temperature kT. The parameters are $\gamma = 0.01$, $a = 1$, $b = -1$, and $N = 20$.

values but also speed up the whole process. For a non-Markovian environment, in the case of the experiment realization, the spin number is typically a more convenient parameter that can be effectively controlled. As such, in order to achieve the maximum spin squeezing, one may try to increase the number of spins to as large as the system permits.

Moreover, in Fig. 3, we study the effects of the environment decay rate Γ and the temperature T on the spin squeezing in the non-Markovian environment. For this purpose, we see that the time range of spin squeezing may be prolonged as the decay rate Γ decreases. The reason is obvious as the weaker decay rates will maintain the system's dynamics longer. On the other hand, choosing different environment temperatures for $kT = 1$, 10, and 100, it shows that the time range of spin squeezing can be narrowed as the temperature T increases. As shown above, the lower environment decay rate or environment temperature will lead to a wider time range of the spin squeezing.

Apart from the above spin numbers, another important feature of the environment is dictated by the parameters a and b, which are shown to be important in spin-squeezing generation. In Fig. 4, we plot the evolution of the spin-squeezing parameter ξ^2 with different ratios a/b and b/a. It is obvious that the spin-squeezing parameter ξ^2 is less than 1 for the time interval from zero to $Jt = 1$ in the low ratios of a/b and b/a (see also Fig. 4). Figure 4(a) shows that the minimum spin squeezing occurs at the point that is close to the ratio $a/b = 0$ and the spin-squeezing parameter ξ^2 is a symmetrical distribution on both sides of $a/b = 0$ with the time evolution. As the ratio a/b increases, we can see, with time development, that the spin-squeezing parameter ξ^2 eventually returns to 1, which means that the spin squeezing is to disappear. This interesting observation may be explained by Eq. (3). In fact, the second term in Eq. (3) represents the nonlinear interaction for the OAT-type spin squeezing, where b is the spin interaction parameter. When $a \sim 0$, it becomes an OAT-type Hamiltonian in the form of $H = bJ_z^2$, which can generate OAT-type spin squeezing as confirmed by the recent spin-squeezing experiment through the state-selective collisions [3–5]. From Fig. 4(b), if we increase the ratio b/a, as the time evolves, the spin-squeezing parameter ξ^2 will exhibit two extreme points located symmetrically around $b/a = 0$. However, we find that the spin-squeezing parameter ξ^2 can be close to 1 when $b/a \sim 0$ for all time points. In the case of $b = 0$, a weakly spin-squeezed state is generated due to the spin relaxation via the Lindblad operator J_-, which was numerically shown in Ref. [34]. Moreover, it also shows that time range of spin squeezing will increase first and then decrease as the ratio b/a increases from 0 to 2. It is shown that spin-squeezing generation begins when the ratio b/a is about 0.3.

V. DISCUSSION AND CONCLUSION

The twist-and-turn model, as special cases of the LMG model, can generate spin squeezing in Bose-Einstein condensation (BEC) systems [23,59–62]. The major advantage of producing spin squeezing in BEC systems is the possible

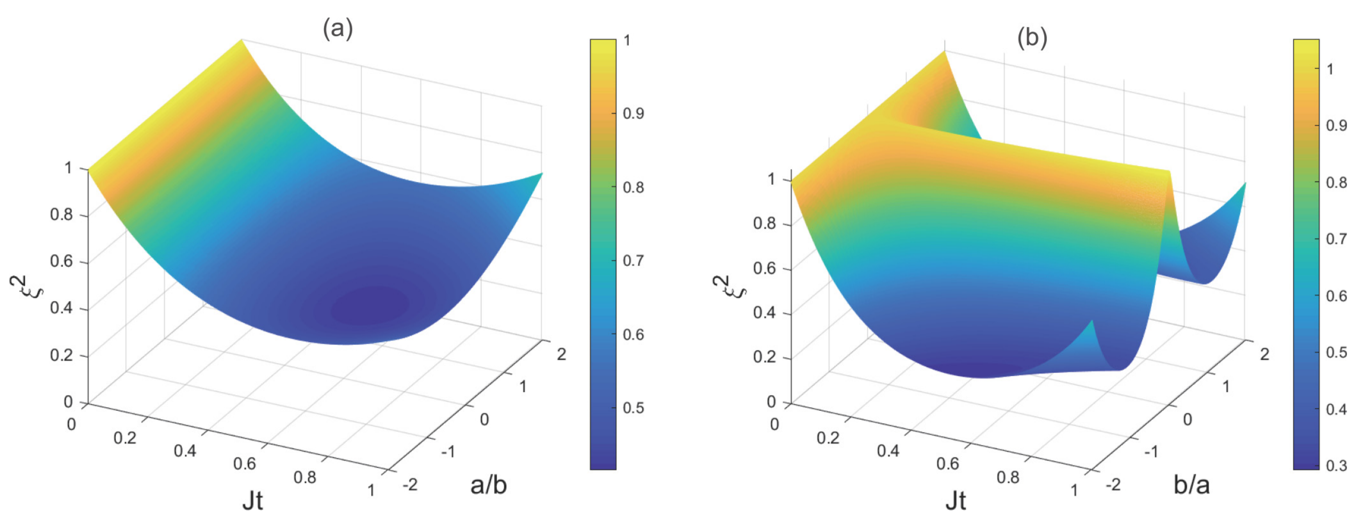

FIG. 4. The time evolution of spin-squeezing parameter ξ^2 with different ratio a/b and different ratio b/a. The parameters are $\Gamma = 0.01$, $\gamma = 2$, $kT = 10$, and $N = 20$.

realization of strong atom-atom interactions, which can induce nonlinearity and squeezing [63–66]. It has been shown that, in the single-mode approximation, the Hamiltonian described in Eq. (3) of N atoms with two internal states $|a\rangle$ and $|b\rangle$ may be realized [67]. A similar Hamiltonian for creating spin squeezing may be also realized with NV centers in diamond [30]. It was demonstrated that the direct spin-phonon coupling in diamond can be used to generate spin-squeezed states of an NV ensemble embedded in the Markov environment. Finally, we note that the Hamiltonian defined in Eq. (3) has been studied in the context of nuclear spins in a quantum dot system [28], where spin squeezing was achieved by using the same OAT Hamiltonian. We emphasize that these physical settings may also be used to realize the non-Markovian spin squeezing after necessary modifications. For example, in the case of a BEC system, it is possible to achieve the strong-coupling regimes for atom-light interaction; therefore, the non-Markovian features discussed here may be studied in these types of systems.

In conclusion, we study the OAT model to generate spin squeezing in the presence of non-Markovian environments at finite temperature. The model is composed of N identical spin-$1/2$ particles interacting with identical bosonic heat baths. We have derived the finite-temperature non-Markovian master equations by using the NMQSD method. In non-Markovian regimes, we numerically investigate the dependence of spin squeezing on several relevant physical parameters including the environment memory times, temperatures, and decay rates. It is shown that the finite memory time scales or large spin numbers can increase both the maximum spin-squeezing values and the squeezing time periods. Moreover, we examine the spin squeezing of the different OAT models corresponding to the different choices of the parameters a and b in Hamiltonian Eq. (3). The results show that, for some parameter domains of a and b, relative strong and long-lived spin squeezing may be obtained.

ACKNOWLEDGMENTS

The project was supported by NSFC (Grant No. 11664029) and the Distinguished Young Scholars Breeding fund of Inner Mongolia (Grant No. 2017JQ08).

APPENDIX A: EVOLUTION EQUATIONS OF OPERATORS O_1 AND O_2

The dynamic equation of O operators could be derived from the consistency conditions

$$\partial_t \frac{\delta\psi_t}{\delta z_s^*} = \frac{\delta}{\delta z_s^*}\partial_t\psi_t, \tag{A1}$$

$$\partial_t \frac{\delta\psi_t}{\delta w_s^*} = \frac{\delta}{\delta w_s^*}\partial_t\psi_t. \tag{A2}$$

Combining the above consistency conditions with the NMQSD Eq. (10), we derive

$$\begin{aligned}\partial_t O_1(t,s,z^*,w^*) = {}& [-iH_{\text{sys}} + Lz_t^* - L^\dagger\bar{O}_1 + L^\dagger w_t^* \\ & - L\bar{O}_2, O_1] - L^\dagger\frac{\delta}{\delta z_s^*}\bar{O}_1 - L\frac{\delta}{\delta z_s^*}\bar{O}_2,\end{aligned} \tag{A3}$$

$$\begin{aligned}\partial_t O_2(t,s,z^*,w^*) = {}& [-iH_{\text{sys}} + Lz_t^* - L^\dagger\bar{O}_1 + L^\dagger w_t^* - L\bar{O}_2, \\ & O_2] - L^\dagger\frac{\delta}{\delta w_s^*}\bar{O}_1 - L\frac{\delta}{\delta w_s^*}\bar{O}_2,\end{aligned} \tag{A4}$$

for $t > s$ along with two initial conditions $O_1(s,s,z^*,w^*) = L$ and $O_2(s,s,z^*,w^*) = L^\dagger$. One can expand O operators in terms of noises,

$$\begin{aligned}O_j(t,s,z^*,w^*) = {}& O_{j,0,0}(t,s) + \int_0^t dv_1 O_{j,1,0}(t,s,v_1)z_{v_1}^* dv_1 \\ & + \int_0^t dv_1' O_{j,0,1}(t,s,v_1')w_{v_1'}^* dv_1' \\ & + \sum_{m,n=1}^{\infty}\int_0^t\cdots\int_0^t dv_1\cdots dv_m\int_0^t\cdots \\ & \times\int_0^t dv_1'\cdots dv_n' O_{j,m,n}(t,s,v_1,\ldots,v_m, \\ & v_1',\ldots,v_n')z_{v_1}^*\cdots z_{v_m}^* w_{v_1'}^*\cdots w_{v_n'}^*,\end{aligned} \tag{A5}$$

where the operators $O_{jmn}(t,s,v_1,\ldots,v_n,v_1',\ldots,v_n')$ are independent of the noises z^* (w^*) and symmetric in their m variables v_k and n variables v_k' with the form

$$\begin{aligned}& O_{j,m,n}(t,s,v_1,\ldots,v_m,v_1',\ldots,v_n') \\ & \quad = O_{j,m,n}(t,s,P_m(v_1),P_m(v_m),P_n(v_1'),\ldots,P_n(v_n')), \\ & \qquad (P_k\in S_k),\end{aligned} \tag{A6}$$

where S_k is a k-element permutation group. By substituting this expansion back into the dynamic equations, we can get

$$\begin{aligned}& \partial_t O_{1,m,n}(t,s,v_1,\ldots,v_m,v_1',\ldots,v_n') \\ & \quad = -i[iH_{\text{sys}}, O_{1,m,n}(t,s,v_1,\ldots,v_m,v_1',\ldots,v_n')] - (m+1)L^\dagger\bar{O}_{1,m+1,n}(t,v_1,\ldots,v_m,v_{m+1}=s,v_1',\ldots,v_n') \\ & \qquad - (m+1)L^\dagger\bar{O}_{2,m+1,n}(t,v_1,\ldots,v_m,v_{m+1}=s,v_1',\ldots,v_n') - \frac{1}{m!n!}\sum_{P_m\in S_m}\sum_{P_n\in S_n}\sum_{k=0}^{m}\sum_{l=0}^{n}[L^\dagger\bar{O}_{1,m-k,n-l} \\ & \qquad \times(t,s,P_m(v_1),\ldots,P_m(v_k),P_n(v_1'),\ldots,P_n(v_l')) + L\bar{O}_{2,m-k,n-l}(t,s,P_m(v_1),\ldots,P_m(v_k),P_n(v_1'),\ldots,P_n(v_l')), \\ & \qquad O_{1,k,l}(t,s,P_m(v_{k+1}),\ldots,P_m(v_m),P_n(v_{l+1}'),\ldots,P_n(v_l'))],\end{aligned} \tag{A7}$$

$$\begin{aligned}
&\partial_t O_{2,m,n}(t,s,v_1,\ldots,v_m,v_1',\ldots,v_n')\\
&= -i[iH_{\rm sys}, O_{2,m,n}(t,s,v_1,\ldots,v_m,v_1',\ldots,v_n')] - (n+1)L^\dagger \bar{O}_{2,m,n+1}(t,v_1,\ldots,v_m,v_1',\ldots,v_n',v_{n+1}'=s)\\
&\quad - (n+1)L^\dagger \bar{O}_{2,m,n+1}(t,v_1,\ldots,v_m,v_1',\ldots,v_n',v_{n+1}'=s)\\
&\quad - \frac{1}{m!n!}\sum_{P_m\in S_m}\sum_{P_n\in S_n}\sum_{k=0}^{m}\sum_{l=0}^{n}[L^\dagger \bar{O}_{1,m-k,n-l}(t,s,P_m(v_1),\ldots,P_m(v_k),P_n(v_1'),\ldots,P_n(v_l'))\\
&\quad + L\bar{O}_{2,m-k,n-l}(t,s,P_m(v_1),\ldots,P_m(v_k),P_n(v_1'),\ldots,P_n(v_l')), O_{2,k,l}(t,s,P_m(v_{k+1}),\ldots,P_m(v_m),P_n(v_{l+1}'),\ldots,P_n(v_l'))],
\end{aligned} \tag{A8}$$

for $t > s$ and initial conditions

$$O_{j,m,n}(t,s,v_1=t,v_2,\ldots,v_m,v_1',\ldots,v_n') = \frac{1}{m}[L, O_{j,m-1,n}(t,s,v_2,\ldots,v_m,v_1',\ldots,v_n')], \tag{A9}$$

$$O_{j,m,n}(t,s,v_1,\ldots,v_m,v_1'=t,v_2',\ldots,v_n') = \frac{1}{n}[L, O_{j,m,n-1}(t,s,v_1,\ldots,v_m,v_2',\ldots,v_n')], \tag{A10}$$

$$O_{j,m,n}(s,s,v_1,\ldots,v_m,v_1',v_2',\ldots,v_n') = \begin{cases} L, & j=1,\ m=0,\ n=0\\ L^\dagger, & j=2,\ m=0,\ n=0\\ 0, & \text{others.}\end{cases} \tag{A11}$$

Note here we introduce the substitutive form $\bar{O}_{j,m,n}(t,v_1,\ldots,v_m,v_1',\ldots,v_n') = \int_0^t ds\alpha_j(t,s)O_{j,m,n}(t,s,v_1,\ldots,v_m,v_1',\ldots,v_n')$ for convenience. When the coupling strength is relatively small ($kT\Gamma \ll a(b)$), a simple but useful approximation for numerical calculations is to truncate the O_j $(j=1,2)$ operators to the zeroth order of noises [56,68], which satisfy the equations:

$$\partial_t O_1(t,s) = [-iH_{\rm sys} - L^\dagger\bar{O}_1(t) - L\bar{O}_2(t), O_1(t,s)], \tag{A12}$$

$$\partial_t O_2(t,s) = [-iH_{\rm sys} - L^\dagger\bar{O}_1(t) - L\bar{O}_2(t), O_2(t,s)]. \tag{A13}$$

APPENDIX B: EXPECTATION OF COLLECTIVE OPERATORS WITH TIME EVOLUTION

In this Appendix, we outline the mean values that enter the variance of Eq. (22). As is known, for an operator $\hat{A}$, the expectation with time evolution can be expressed by means of the master equation as $d\langle\hat{A}\rangle/dt = \mathrm{tr}[\hat{A}\dot{\rho}]$. Using Eq. (20) we can easily obtain the following equations,

$$\frac{d}{dt}\langle A\rangle = -i\langle[A,H_{\rm sys}]\rangle + \{\langle\bar{O}_1^\dagger[A,L]\rangle + \langle[L^\dagger,A]\bar{O}_1\rangle + \langle\bar{O}_2^\dagger[A,L^\dagger]\rangle + \langle[L,A]\bar{O}_2\rangle\}, \tag{B1}$$

$$\frac{d}{dt}\langle J_-\rangle = -i(a+b)\langle J_-\rangle - 2ib\langle J_zJ_-\rangle + \{2F_{11}(\langle J_zJ_-\rangle) - 2F_{21}^*(\langle J_zJ_-\rangle + \langle J_-\rangle) - 2F_{22}^*(\langle J_zJ_-\rangle + \langle J_z^2J_-\rangle)\}, \tag{B2}$$

$$\begin{aligned}
\frac{d}{dt}\langle J_z\rangle = 2\mathrm{Re}\{&-F_{11}^*(J(J+1) - \langle J_z^2\rangle + \langle J_z\rangle) - F_{12}^*(-J(J+1) + (J(J+1)-1)\langle J_z\rangle + 2\langle J_z^2\rangle - \langle J_z^3\rangle)\\
&+F_{21}^*(J(J+1) - \langle J_z^2\rangle - \langle J_z\rangle) + F_{22}^*(J(J+1) + (J(J+1)-1)\langle J_z\rangle - 2\langle J_z^2\rangle - \langle J_z^3\rangle)\},
\end{aligned} \tag{B3}$$

$$\begin{aligned}
\frac{d}{dt}\langle J_-^2\rangle = &-i(2a+4b)\langle J_-^2\rangle - 4ib\langle J_zJ_-^2\rangle + F_{11}(4\langle J_zJ_-^2\rangle + 2\langle J_-^2\rangle) + F_{12}(4\langle J_z^2J_-^2\rangle\\
&+6\langle J_zJ_-^2\rangle + 2\langle J_-^2\rangle) - F_{21}^*(4\langle J_zJ_-^2\rangle + 6\langle J_-^2\rangle) - F_{22}^*(4\langle J_z^2J_-^2\rangle + 6\langle J_zJ_-^2\rangle),
\end{aligned} \tag{B4}$$

$$\begin{aligned}
\frac{d}{dt}\langle J_z^2\rangle = 2\mathrm{Re}\{&-F_{11}^*(-J(J+1) + (2J(J+1)-1)\langle J_z\rangle + 3\langle J_z^2\rangle - 2\langle J_z^3\rangle)\\
&-F_{12}^*(J(J+1) - (3J(J+1)-1)\langle J_z\rangle + (2J(J+1)-4)\langle J_z^2\rangle + 5\langle J_z^3\rangle - 2\langle J_z^4\rangle)\\
&+F_{21}^*(J(J+1) + (2J(J+1)-1)\langle J_z\rangle - 3\langle J_z^2\rangle - 2\langle J_z^3\rangle)\\
&+F_{22}^*(J(J+1)\langle J_z\rangle + (2J(J+1)-1)\langle J_z^2\rangle - 3\langle J_z^3\rangle - 2\langle J_z^4\rangle)\},
\end{aligned} \tag{B5}$$

$$\begin{aligned}\frac{d}{dt}\langle J_zJ_-\rangle = &-ia\langle J_zJ_-\rangle - ib\big(\langle J_zJ_-\rangle + 2\big\langle J_z^2J_-\big\rangle\big) + \big\{ - F_{11}\big(J(J+1)\langle J_-\rangle + \langle J_zJ_-\rangle - 3\big\langle J_z^2J_-\big\rangle\big)\\ &-F_{11}^*\big(J(J+1)\langle J_-\rangle + \langle J_zJ_-\rangle - \langle J_z^2J_-\rangle\big) - F_{12}\big(J(J+1)\langle J_zJ_-\rangle + \langle J_z^2J_-\rangle - 3\big\langle J_z^3J_-\big\rangle\big)\\ &- F_{12}^*\big(- J(J+1)\langle J_-\rangle + (J(J+1)-1)\langle J_zJ_-\rangle + 2\big\langle J_z^2J_-\big\rangle - \big\langle J_z^3J_-\big\rangle\big) + F_{21}\big((J(J+1)-2)\langle J_-\rangle\\ &-3\langle J_zJ_-\rangle - \big\langle J_z^2J_-\big\rangle\big) + F_{21}^*\big((J(J+1)-2)\langle J_-\rangle - 5\langle J_zJ_-\rangle - 3\big\langle J_z^2J_-\big\rangle\big)\\ &+F_{22}\big((J(J+1)-2)\langle J_-\rangle + (J(J+1)-5)\langle J_zJ_-\rangle - 4\big\langle J_z^2J_-\big\rangle - \big\langle J_z^3J_-\big\rangle\big)\\ &+F_{22}^*\big((J(J+1)-2)\langle J_zJ_-\rangle - 5\big\langle J_z^2J_-\big\rangle - 3\big\langle J_z^3J_-\big\rangle\big)\big\}.\end{aligned} \tag{B6}$$

[1] D. J. Wineland, J. J. Bollinger, W. M. Itano, and D. J. Heinzen, Phys. Rev. A **50**, 67 (1994).
[2] M. Kitagawa and M. Ueda, Phys. Rev. A **47**, 5138 (1993).
[3] J. Esteve, C. Gross, A. Weller, S. Giovanazzi, and M. K. Oberthaler, Nature (London) **455**, 1216 (2008).
[4] C. Gross, T. Zibold, E. Nicklas, J. Esteve, and M. K. Oberthaler, Nature (London) **464**, 1165 (2010).
[5] M. F. Riedel, P. Böhi, Y. Li, T. W. Hönsch, A. Sinatra, and P. Treutlein, Nature (London) **464**, 1170 (2010).
[6] H. F. Hofmann and S. Takeuchi, Phys. Rev. A **68**, 032103 (2003).
[7] G. Toth, C. Knapp, O. Guhne, and H. J. Briegel, Phys. Rev. A **79**, 042334 (2009).
[8] E. G. Cavalcanti, P. D. Drummond, H. A. Bachor, and M. D. Reid, Opt. Express **17**, 18693 (2009).
[9] E. G. Cavalcanti, S. J. Jones, H. M. Wiseman, and M. D. Reid, Phys. Rev. A **80**, 032112 (2009).
[10] M. D. Reid, P. D. Drummond, W. P. Bowen, E. G. Cavalcanti, P. K. Lam, H. A. Bachor, U. L. Andersen, and G. Leuchs, Rev. Mod. Phys. **81**, 1727 (2009).
[11] K. Hammerer, E. S. Polzik, and J. I. Cirac, Phys. Rev. A **72**, 052313 (2005).
[12] A. Sørensen, L. Duan, J. Cirac, and P. Zoller, Nature (London) **409**, 63 (2001).
[13] N. Bigelow, Nature (London) **409**, 27 (2001).
[14] O. Guehne and G. Tóth, Phys. Rep. **474**, 1 (2009).
[15] D. J. Wineland, J. J. Bollinger, W. M. Itano, F. L. Moore, and D. J. Heinzen, Phys. Rev. A **46**, R6797(R) (1992).
[16] E. S. Polzik, Nature (London) **453**, 45 (2008).
[17] A. D. Cronin, J. Schmiedmayer, and D. E. Pritchard, Rev. Mod. Phys. **81**, 1051 (2009).
[18] A. Louchet-Chauvet, J. Appel, J. J. Renema, D. Oblak, N. Kjaergaard, and E. S. Polzik, New J. Phys. **12**, 065032 (2010).
[19] I. D. Leroux, M. H. Schleier-Smith, and V. Vuletić, Phys. Rev. Lett. **104**, 250801 (2010).
[20] J. Appel *et al.*, Proc. Natl. Acad. Sci. USA **106**, 10960 (2009).
[21] M. H. Schleier-Smith, I. D. Leroux, and V. Vuletić, Phys. Rev. Lett. **104**, 073604 (2010); Phys. Rev. A **83**, 039907(E) (2011).
[22] M. E. Tasgin and P. Meystre, Phys. Rev. A **83**, 053848 (2011).
[23] W. Muessel, H. Strobel, D. Linnemann, T. Zibold, B. Juliá-Díaz, and M. K. Oberthaler, Phys. Rev. A **92**, 023603 (2015).
[24] E. G. DallaTorre, J. Otterbach, E. Demler, V. Vuletić, and M. D. Lukin, Phys. Rev. Lett. **110**, 120402 (2013).
[25] M. Saffman, D. Oblak, J. Appel, and E. S. Polzik, Phys. Rev. A **79**, 023831 (2009).
[26] A. Kuzmich, K. Mølmer, and E. S. Polzik, Phys. Rev. Lett. **79**, 4782 (1997).
[27] J. Hald, J. L. Sørensen, C. Schori, and E. S. Polzik, Phys. Rev. Lett. **83**, 1319 (1999).
[28] M. S. Rudner, L. M. K. Vandersypen, V. Vuletić, and L. S. Levitov, Phys. Rev. Lett. **107**, 206806 (2011).
[29] Y. A. Korkmaz and C. Bulutay, Phys. Rev. A **93**, 013812 (2016).
[30] S. D. Bennett, N. Y. Yao, J. Otterbach, P. Zoller, P. Rabl, and M. D. Lukin, Phys. Rev. Lett. **110**, 156402 (2013).
[31] Y. H. Ma and X. F. Zhang, Phys. Rev. B **89**, 144113 (2014).
[32] Y. H. Ma, X. F. Zhang, J. Song, and E. Wu, Ann. Phys. **369**, 36 (2016).
[33] G. Feher, Phys. Rev. **114**, 1219 (1959).
[34] S. Dooley, E. Yukawa, Y. Matsuzaki, G. C. Knee, W. J. Munro, and K. Nemoto, New J. Phys. **18**, 053011 (2016).
[35] A. E. B. Nielsen and K. Mølmer, Phys. Rev. A **77**, 063811 (2008).
[36] J. Doukas and L. C. L. Hollenberg, Phys. Rev. A **79**, 052109 (2009).
[37] T. E. Lee and C. K. Chan, Phys. Rev. A **88**, 063811 (2013).
[38] H. Saito and M. Ueda, Phys. Rev. A **68**, 043820 (2003).
[39] X. G. Wang, A. Miranowicz, Y. X. Liu, C. P. Sun, and F. Nori, Phys. Rev. A **81**, 022106 (2010).
[40] X. Yin, J. Ma, X. G. Wang, and F. Nori, Phys. Rev. A **86**, 012308 (2012).
[41] G. M. Moy, J. J. Hope, and C. M. Savage, Phys. Rev. A **59**, 667 (1999).
[42] I. de Vega and D. Alonso, Phys. Rev. A **77**, 043836 (2008).
[43] Y. N. Chen, G. Y. Chen, Y. Y. Liao, N. Lambert, and F. Nori, Phys. Rev. B **79**, 245312 (2009).
[44] S. John and T. Quang, Phys. Rev. Lett. **74**, 3419 (1995).
[45] S. Bay, P. Lambropoulos, and K. Mølmer, Phys. Rev. A **57**, 3065 (1998).
[46] N. Vats and S. John, Phys. Rev. A **58**, 4168 (1998).
[47] T. Ma, Y. Chen, T. Chen, S. R. Hedemann, and T. Yu, Phys. Rev. A **90**, 042108 (2014).
[48] L. Diósi, N. Gisin, and W. T. Strunz, Phys. Rev. A **58**, 1699 (1998).
[49] W. T. Strunz, L. Diósi, and N. Gisin, Phys. Rev. Lett. **82**, 1801 (1999).

[50] T. Yu, L. Diósi, N. Gisin, and W. T. Strunz, Phys. Rev. A **60**, 91 (1999).
[51] H. J. Lipkin, N. Meshkov, and A. J. Glick, Nucl. Phys. **62**, 188 (1965).
[52] R. Botet, R. Jullien, and P. Pfeuty, Phys. Rev. Lett. **49**, 478 (1982).
[53] J. I. Cirac, M. Lewenstein, K. Mølmer, and P. Zoller, Phys. Rev. A **57**, 1208 (1998).
[54] D. I. Tsomokos, S. Ashhab, and F. NoriNew J. Phys. **10**, 113020 (2008).
[55] J. Ma and X. Wang, Phys. Rev. A **80**, 012318 (2009).
[56] T. Yu, Phys. Rev. A **69**, 062107 (2004); W. T. Strunz and T. Yu, *ibid.* **69**, 052115 (2004).
[57] J. Jing, R. Li, J. Q. You, and T. Yu, Phys. Rev. A **91**, 022109 (2015).
[58] J. Ma, X. G. Wang, C. P. Sun, and F. Nori, Phys. Rep. **509**, 89 (2011).
[59] W. Huang, Y. L. Zhang, C. L. Zou, X. B. Zou, and G. C. Guo, Phys. Rev. A **91**, 043642 (2015).
[60] J. Grond, G. von Winckel, J. Schmiedmayer, and U. Hohenester, Phys. Rev. A **80**, 053625 (2009).
[61] G. R. Jin and C. K. Law, Phys. Rev. A **78**, 063620 (2008).
[62] G. R. Jin and S. W. Kim, Phys. Rev. Lett. **99**, 170405 (2007).
[63] S. Thanvanthri and Z. Dutton, Phys. Rev. A **75**, 023618 (2007).
[64] S. D. Jenkins and T. A. B. Kennedy, Phys. Rev. A **66**, 043621 (2002).
[65] D. Jaksch, J. I. Cirac, and P. Zoller, Phys. Rev. A **65**, 033625 (2002).
[66] U. V. Poulsen and K. Molmer, Phys. Rev. A **64**, 013616 (2001).
[67] A. S. Sørensen, Phys. Rev. A **65**, 043610 (2002).
[68] J. Xu, X. Y. Zhao, J. Jing, L. A. Wu, and T. Yu, J. Phys. A **47**, 435301 (2014).